GOES-R Risk Reduction Program

Progress Report for July – September 2006
from the
University of Wisconsin-Madison
Cooperative Institute for Meteorological Satellite Studies

Project Title:	CIMSS Participation in GOES-R Risk Reduction
Principle Investigator:	Steve Ackerman
Co-Investigators:	Allen Huang (Algorithms), Chris Velden (Winds),
	Elaine Prins, Chris Schmidt (Fires),
	Jim Kossin (Tropical Cyclones) Ralph Petersen (Nowcasting),
	Bob Knuteson (Data Systems), Dave Tobin (Validation)
Additional Contributors:	Jun Li, Xiolie Zhou (FSU), Ray Garcia
Program Manager:	Tom Achtor
Date:	September 2006
FY2006 Funding:	$1,400,000
Remaining Funds:	$458,000 (through December 2006)

Topics Summary

Program Management and Coordination

Refer to the dedicated internal web site (http://cimss.ssec.wisc.edu/goes_r/rr/) for information concerning management and coordination:
- GOES-R3 AD monthly meeting
- Monthly reports
- Group quarterly reports
- Meeting minutes, and
- Announcements.

Task 1. Algorithm Development

1.1. Sounding Retrievals Algorithm Development
Lead Investigator: Allen Huang

Study on the simultaneous retrieval of emissivity spectrum along with temperature and moisture soundings in clear sky
Figure 1 shows the true emissivity (black) used to calculate the AIRS radiances (with noise included), emissivity first guess from regression (red), physical retrieval of emissivity if temperature and moisture soundings are known (blue), and the physical retrieval of emissivity if temperature and moisture soundings are unknown (green). The blue line shows that if the temperature and moisture soundings are known, the detailed structure of emissivity spectrum can be retrieved very well. This demonstrates that the emissivity information contained in the radiance spectrum and is retrievable. Since the temperature and moisture soundings also need to be retrieved, the green line is more representative of the reality; the retrieved emissivity spectrum still fits truth well, although there is degradation on fine structure retrieval.
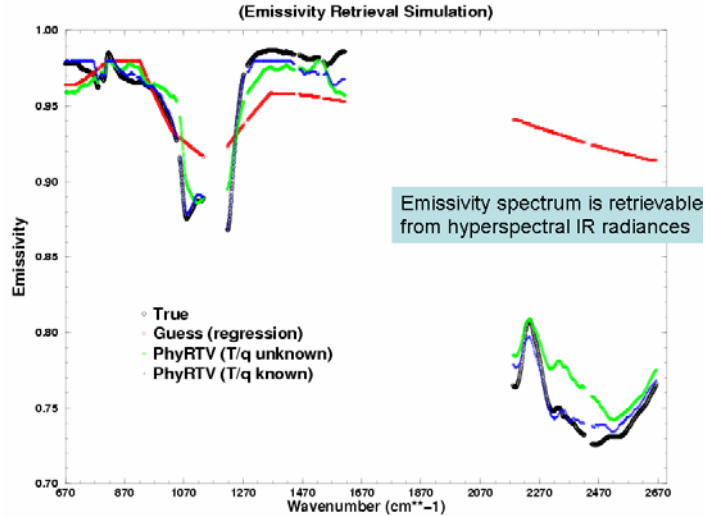
Figure 1. The true emissivity (black) used to calculate the AIRS radiances (with noise included), first guess from regression (red), physical retrieval of emissivity if temperature and moisture soundings are known (blue), and the physical retrieval of emissivity if temperature and moisture soundings are unknown (green).

The next step is to apply the algorithm to real AIRS data; the regression technique has been upgraded using the new training data (Seemann et al. 2006, submitted to JAM). Figure 2 shows an AIRS brightness temperature (BT) image of 8.2 µm (upper left) and the emissivity regression retrieval at 8.3 µm (upper right). The emissivity over desert regions is lower than 0.85, which is consistent with what we observed from laboratory measurements. This regression will be further improved by the physical approach mentioned above.
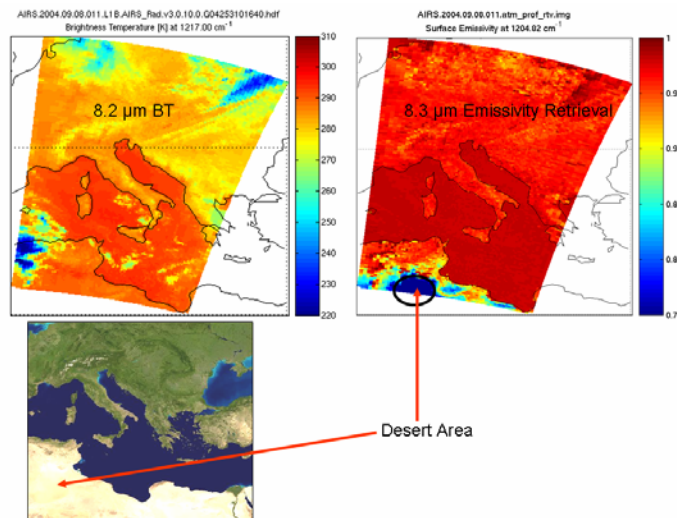

Figure 2. An AIRS BT image of 8.2 µm (upper left) and the emissivity regression retrieval at 8.3 µm (upper right).

Study of ABI ozone retrieval algorithm
An algorithm has been developed for the Advanced Baseline Imager (ABI), and tested using the Spinning Enhanced Visible and Infra-Red Imager (SEVIRI) onboard Meteosat-8. Simulation shows that Ozone accuracy from SEVIRI is worse than that from the current GOES Sounder due to lack of stratospheric CO_2 absorption spectral bands in SEVIRI. However, with the help of

temperature profiles from forecast, the SEVIRI/ABI provides Ozone with similar accuracy of the current GOES Sounder (Jin et al. 2006, to be submitted to IEEE TGARS) but with much larger spatial coverage (disk). Preliminary results show that the total column Ozone retrievals from SEVIRI agree well with ozone measurements from Ozone Monitoring Instrument (OMI) onboard the Earth Observing System's Aura platform. Figure 3 shows the OMI (upper) and SEVIRI (lower) total column ozone measurements in clear skies from 15 to 16 February 2006 over Europe. OMI provides global ozone once every day while SEVIRI provides ozone in disk coverage every 15 minutes. In addition, SEVIRI with 15-minute temporal resolution depicts the ozone transportation and evolution very well.
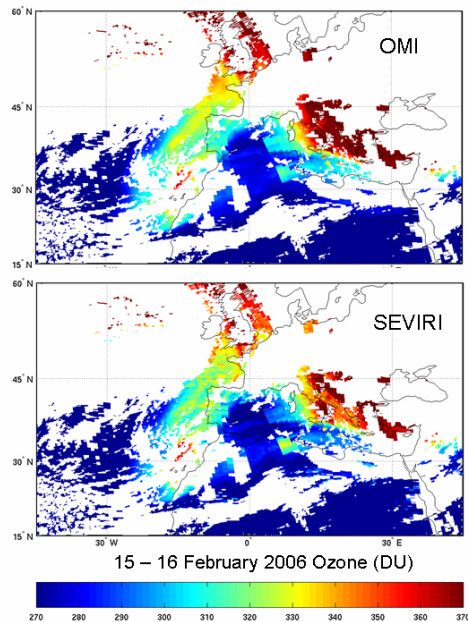

Figure 3. The scatter plot of OMI (upper) and SEVIRI (lower) total column ozone measurements in clear skies over Europe from 15 to 16 February 2006. SEVIRI agrees well with OMI.

Surface Emissivity Study and Modeling

The work in this quarter focused on 1) improving upon the moderate spectral resolution land surface emissivity (LSE) database ("baseline fit" approach, previously called "version A"), 2) finalizing and submitting a paper detailing the derivation of the database and its application to AIRS and MODIS temperature and moisture retrievals, and 3) comparing this dataset with other emissivity databases derived from MSG/SEVIRI and Aqua/AIRS satellite data.

During this quarter, a second version of the moderate spectral resolution land surface emissivity database (derived by baseline spectral fit to MOD11 points) was released and is available from the CIMSS website (**http://cimss.ssec.wisc.edu/iremis**). This updated version includes improvements to the baseline fitting procedure, emissivity values at 10 (wavelength) inflection points, and a more user-friendly NetCDF data format. A registration procedure has been set up to monitor access to the database on the CIMSS website.

In this quarter the paper describing this database was also submitted to Journal of Applied Meteorology and Climatology. After distributing the database and submitting the paper the work focused on the comparison of this database with other emissivity datasets. Preliminary work has been done to compare three infrared land surface emissivity databases.

The BF LSE database and the operational AIRS emissivity retrievals were compared at 42 wavelengths for July 2004. BF LSE database values that fell inside of the AIRS emissivity retrieval FOVs were averaged. Monthly mean differences, the ratio of the differences and the histogram of the values was calculated. The comparison of the BF database with the SAF database was made for 2006 January in 4 regions of the world at 4 wavelengths (3.9, 8.7, 10.8, 12.0 µm, SAF spectral resolution). This time, the SAF database grid was interpolated onto the BF database grid. The analysis of the comparison of these three databases is under process, and two selected comparisons are shown below. Figure 4 shows the monthly mean differences between the SEVIRI and BF emissivities at 8.7 microns in North Africa for January 2006. Figure 5 shows the differences between the AIRS and BF emissivities globally at 8.5 microns.
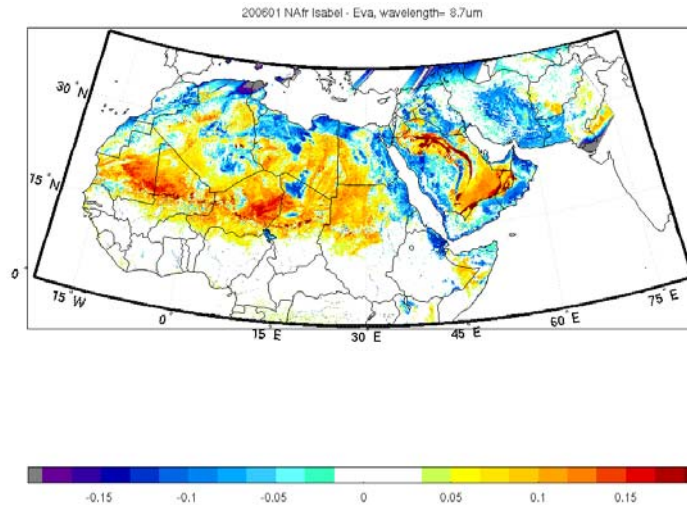

Figure 4: Monthly mean differences between the SAF/SEVIRI and BF emissivities at 8.7 microns in North Africa for January 2006
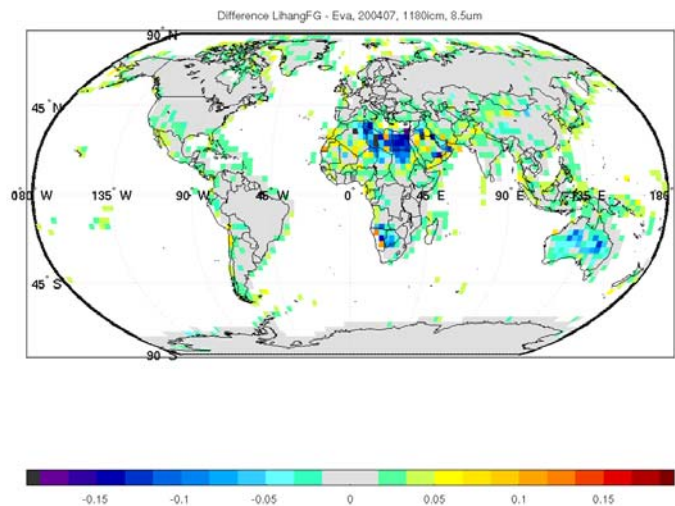

Figure5: Monthly mean differences between the AIRS and BF emissivities globally at 8.5 microns for July 2004.

Cloudy Fast Forward Model Development
- Comparisons of the fast model results against the reference model for 1440 WRF-simulated atmospheric/cloud profiles revealed that for clouds with visible optical depths less than 10 (where errors are expected to be the greatest), scattering errors in terms of brightness temperature at nadir had biases less than 0.5 K across the spectrum and the RMSE's were under 1.5 K (see figure). For a much larger zenith angle the bias errors increased to less than 1 K (RMSE < 2 K).
- We have developed a new version of the fast radiative transfer equation solver based on the adding/doubling principles, which, after combining with a fast clear-sky spectral model, can be applied to the simulation of the hyperspectral radiances observed at the top of the atmosphere under cloudy conditions. Figure 6 shows the spectra simulated for ice clouds. We have been working on further improvement of the efficiency and accuracy of this radiative transfer solver.
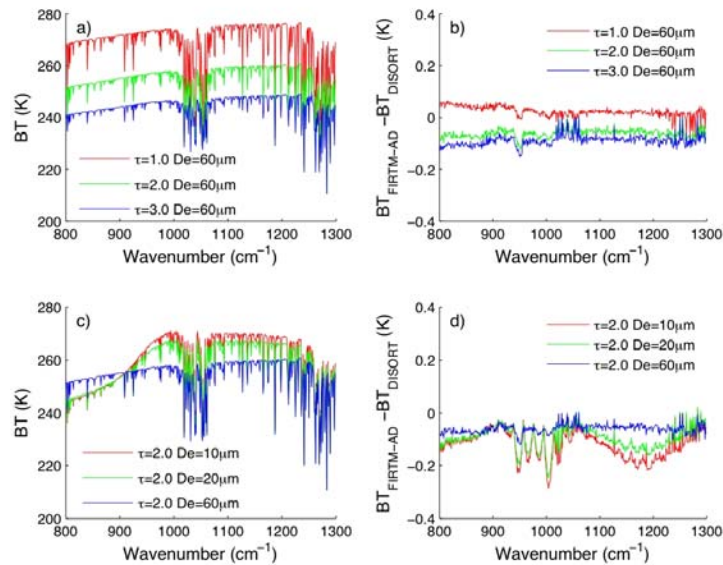

Fig. 6. High-resolution brightness temperature (BT) spectra at TOA computed from the present fast hyperspectral radiative transfer model. Also shown are the corresponding errors with respect to the results from a discrete-ordinate radiative transfer model. A tropical atmosphere was used in the computation. The cloud top pressure of a single-layered ice cloud is 217hp. The temperature and emissivity of the surface are 299.7 K and 0.97, respectively.

Soundings Summary of Significant Inputs in the last three months
- Simultaneous retrieval of profile and surface emissivity spectrum in eigenvector domain algorithm was tested .
- Continued to refine global emissivity database and make comparisons with other available datasets.
- Published surface emissivity dataset paper.
- Continued to improve and incorporate new features to high spectral resolution cloudy sky forward model.

Recent presentations & publications:
Suzanne W. Seemann, Eva E. Borbas, Robert O. Knuteson, Elisabeth Weisz, Gordon R. Stephenson, Jun Li, Hung Lung Huang: A global infrared surface emissivity database for clear

sky atmospheric sounding retrievals from satellite-based radiance measurements. (Submitted for publication to Journal of Applied Meteorology and Climatology).

Zhang, Z., P. Yang, H.-L. Huang, B. A. Baum, and D. Zhou: A fast radiative transfer model for hyperspectral remote sensing,12th Conference on Cloud Physics/12th Conference on Atmospheric Radiation, Madison, Wisconsin, July 10-14, 2006

Hong, G., P. Yang, H.-L. Huang, B. A. Baum, Y. X. Hu, and S. Platnick. Influence of cloud geometrical thickness on the estimate of ice cloud optical thickness and effective particle size using satellite multispectral measurements, 12th Conference on Cloud Physics/12th Conference on Atmospheric Radiation, Madison, Wisconsin, July 10-14, 2006.

Lee, Y.-K., P. Yang, H.-L. Huang, B. A. Baum, and Y. Hu: Retrieval of ice cloud properties using hyperspectral infrared channel observations, 12th Conference on Cloud Physics/12th Conference on Atmospheric Radiation, Madison, Wisconsin, July 10-14, 2006

1.2.   *GOES-R Winds Work Summary*
Lead Investigator: Chris Velden

Previous GOES-R Risk Reduction winds work concentrated on demonstrating the ability to target and track features from WRF model moisture fields and simulated moisture retrievals. The ATReC and Ocean Winds datasets were used. However, the data staging process involved many steps and was labor intensive. The next dataset to be investigated (FULLDISK) dwarfs the previous two cases in the number and size of files. It was determined that the current data staging routines were inadequate for the FULLDISK simulation.

To address the needs of the winds software, a new approach to creating the imagery (McIDAS AREA format) has been implemented. The software is still evolving, but has proven to work for the Ocean Winds dataset. It will need revisions to work with the FULLDISK simulation.

WRF simulations are broken up into "cubes" to simulate HES. These cubes are written as Unidata network Common Data Form (NetCDF) files. Each NetCDF file contains the moisture field information. The new data staging code uses Jython to stitch the cubes together into a McIDAS AREA file. Jython is an implementation of Python integrated with the Java platform.

Significant Accomplishments in the last three months
Jython code to create McIDAS AREA files from NetCDF files was successfully tested.

Plans for Next Three Months
The Jython code will be modified, along with the existing winds software as part of an upcoming SSEC/CIMSS demonstration of the GOES-R data processing system.

1.3.   *Biomass Burning Research*
Lead Investigators: Elaine Prins, Chris Schmidt

The UW-Madison burning team proposed the following tasks:

Research and development activities in 2006 are centered primarily on active fire product development and validation. Development is focused on active fire detection and sub-pixel characterization for emission estimates, including the investigation of fire radiative power. This effort involves the use of multiple data sources (geo and leo) that take advantage of the strengths of each system to create improved fused fire products. This risk reduction activity ensures enhanced future fire detection, monitoring and characterization. Initially CIMSS is investigating GOES ABI fire monitoring capabilities by simulating ABI with MODIS, MSG (METEOSAT Second Generation), and MTSAT-1R (Multi-functional Transport SATellite) multispectral data.

Accomplishments:
To date CIMSS efforts to simulate GOES-R ABI data from higher spatial resolution MODIS data have consisted of applying simple averaging or point spread functions to higher resolution MODIS data in the native MODIS projection. In order to create more realistic GOES-R ABI data sets that can be used to develop improved fire detection and sub-pixel characterization, it is necessary to take into consideration point spread function and oversampling issues, variations in pixel size with view angle, diffraction, band-to-band co-registration, and other factors. These are issues which strongly impact fire detection and sub-pixel characterization. CIMSS is investigating ways to simulate more realistic ABI data utilizing MODIS, Met-8 SEVIRI and GOES data. For a given region of interest the MODIS and coincident GOES/Met-8 data can serve as bookends over a period of time with GOES and Met-8 providing the diurnal signature. At the bookends, the MODIS data can be made to look more like the SEVIRI/GOES data at a higher ABI resolution and then nudged over time (between the bookends) with guidance from the GOES/MET-8 data. Since fires can often appear as an on/off type feature, the diurnal GOES/Met-8 data can be used to introduce variation in fire location and intensity over time. It would also be possible to use an educated random fire generator for certain biomes.

CIMSS is investigating the possibility of modifying existing McIDAS code to create these enhanced more realistic simulated data sets for all ABI IR channels that have similar MODIS channels. Although the band widths for ABI and MODIS can be quite different, this type of simulation would provide "real world" proxy data that can be used in conjunction with model simulated data, with applications in various product development activities. The McIDAS remapping software could possibly be modified to take into consideration factors such as point spread function and oversampling, view angle dependencies, diffraction, band-to-band co-registration, etc. As a first step we will remap MODIS 1 km data into a high resolution GOES projection that will then be modified to take into consideration these additional factors. CIMSS is focusing on simulating GOES ABI from MODIS data collected on 24 April 2004 in Central America. This case study includes excellent examples of diurnal variability in fire activity in both clear and cloudy situations.

During the past quarter NOAA/NESDIS indicated that there was a possibility of obtaining 2 km MTSAT-1R JAMI data for specific case studies. Obtaining access to this data set would provide a wonderful opportunity to investigate the lower thresholds for GOES-R fire detection and monitoring capabilities from a large detector array with a spatial resolution similar to ABI. CIMSS provided input to NOAA/NESDIS regarding priorities for MTSAT-1R 2 km data coverage.

1.4. Tropical Cyclone Research
Lead Investigator: Jim Kossin

We have been following two objectives: the first objective in the initial phase of our GOES-R risk reduction work was to utilize *in situ* data collected by aircraft reconnaissance missions into TCs to make formal comparisons with retrieved products (simulated HES measurements from both real and model-generated synthetic data fields) and determine error correlations in both the cloudy and clear regions of the TC environment. Our first task was to choose a suitable test-case. Working with Mike Black at the NOAA Hurricane Research Division (HRD), and members of the CIMSS retrieval team (Elisabeth Weisz and Yong-Keun Lee), we studied the lists of archived soundings from G4 aircraft sorted into hurricanes and matched the dates/times/positions with available AIRS granules. We identified two hurricanes (Ivan and Frances 2004) with around 215 dropsondes that were spatially and temporally collocated with the AIRS data. These data will be combined with data being constructed at CIRA/CSU – for the mutual benefit of both CIMSS and CIRA, who are applying the data to a different problem. We are presently in the process of obtaining the dropsonde data from HRD, and we will quantify error characteristics after this step.

A second objective of our GOES-R risk reduction work is to demonstrate what will be achievable with the availability of the ABI. One way to do this is to employ currently existing GOES observing strategies that mimic what will be possible with ABI. Specifically, in regards to tropical cyclones, the upper-level outflow is thought to be important toward understanding intensity change. Atmospheric motion vectors (AMVs), derived from special GOES five-minute rapid-scan (r/s) imaging operations, can be effective at simulating what will be available on a routine basis once GOES-R is launched.

As a demonstration of this capability, GOES-11 AMVs were derived from 5-min. r/s imagery during a special observing period as NASA's Tropical Cloud Systems and Processes (TCSP) experiment was taking place in July of 2005. Hurricane Emily traversed the sampling domain and provides a good case study, as the intensity fluctuated during the period of observation. Upper-level divergence is one parameter often associated with intensity change. Divergence from a particular analysis, calculated on spherical coordinates, is shown in figure 7. The wind observations (in ms^{-1}) are also plotted. The divergence was only calculated for points that have at least two observations within 0.25 degrees of the analysis point in order to avoid spurious divergence features created by the analysis scheme. The analysis in figure 7 captures some of the upper-level divergence over the hurricane (100 kits max wind at the analysis time). This divergence precedes Emily strengthening to 130 kits over the subsequent twenty-four hours.

We plan to create time series of upper-level quantities derived from the GOES r/s AMVs over Emily. From these we hope to denote trends and potentially associations with the hurricane's structure and intensity fluctuations. High-resolution data such as this will be routinely possible from the GOES-R ABI, and our intent is to see what we can observe and learn from current GOES capabilities (special observing modes) in advance of this deployment.
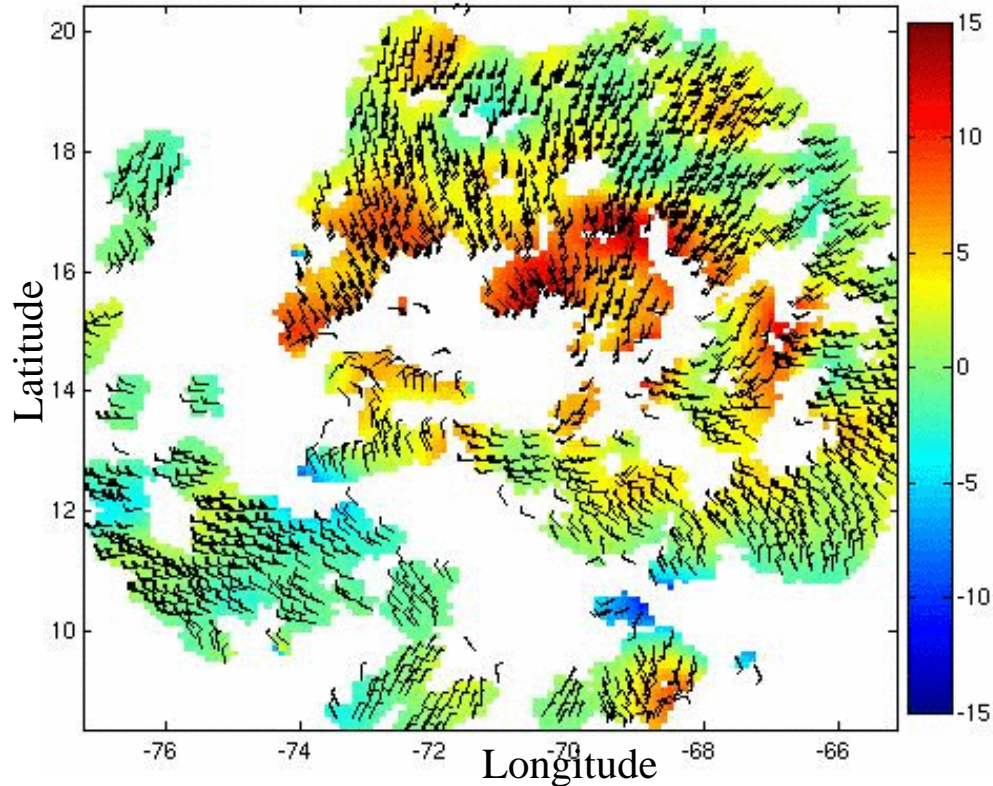
Figure 7: Divergence (10^5 s^{-1}) analysis centered on hurricane Emily valid 16z on 15 July, 2005.

Task 2: Nowcasting
Lead Investigator: Ralph Petersen

1) Work continued in all 4 proposed areas, focusing on the ability of GOES moisture data to identify development of areas of convective instability 3-6 hours in advance of storm development. Ongoing tests with existing GOES sounder DPI data provide a lower-spatial resolution surrogate for GOES-R ABI data. Tests using AIRS data to assess the added impact of improved vertical resolution from a GOES sounder in NWP are being de-emphasized with the decision to eliminate HES from the GOES-R series, although experiments using AIRS data in nowcasting are still planned. Training sessions to allow NWS forecasters to assess nowcasting products are being scheduled so that evaluations can begin during next year's severe storm season..

2) Summary of accomplishments and findings for 1 July through 30 September 2006 by task:
a) Development of visualization tools to detect potential for development of convection: Work continued to improve tools for anticipating development of severe thunderstorms, especially hard-to-forecast isolated severe events. Although development of the nowcasting model itself has already occurred, recent efforts focused on developing visualization tools and web presentation capabilities that allow forecaster to easily integrate DPI observations and nowcasts into their forecasting procedures. A prototype nowcast web page showing nowcasts for a 13 April 2006 WI hail event are available at http://cimss.ssec.wisc.edu/model/ncstR_13Apr06/nowcast.html . It includes hourly animations of DPI-like images of mid- and high-level precipitable water and derived vertical moisture gradients (a necessary condition for convective instability), along with verification satellite imagery. All of the image products now 'cycle' upon each other, in that each

nowcast image uses a contemporaneous image from the previous hourly nowcast run as a 'first-guess', thereby increasing resolution and retaining past data in new products.

Additional tests were made using data for the 13 April 2006 hail storms, which tracked from south of MSN to west of MKE and caused millions of dollars of property damage. Although the standard NWP guidance from the NAM model showed no evidence to this storm development, the nowcast system transported the low-level moisture observed in the initial DPI data over central IA into an isolated band extending across south-central WI within 6 hours, while simultaneously overlaying a narrow area of mid-level dryness originating over south-western MN. Derived vertical moisture differences show an initial development of isolated instability (dark blue to bright red area) over central IA at the time of a tornado sighting there, followed by rapid development of instability over extreme southern WI by 6 hours into the nowcast, when and where the hail storms developed. The results clearly show both the value of multi-layer moisture data from GOES and the ability of the nowcast system to retain and project isolated moisture extremes in anticipation of hard-to-forecast convective events. In an effort both to make the stability calculations more exact and to incorporate the effects of localized diurnal heating noted by GOES data, the nowcasting system will be expanded during the next quarter to include multi-layer predictions of Equivalent Potential Temperature (2e) and vertical differences (convective instability).
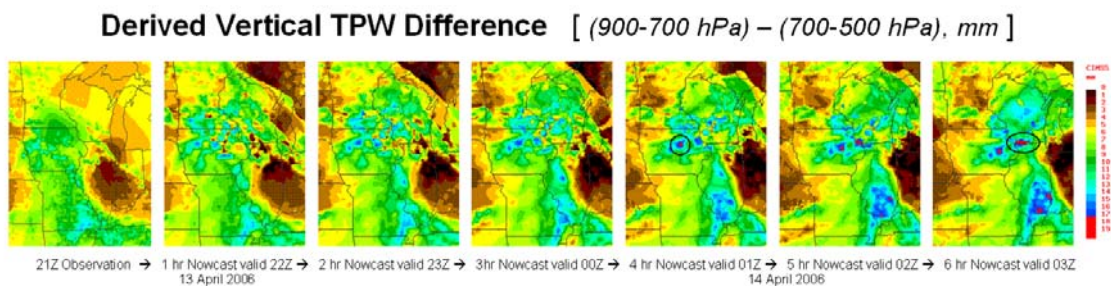

Figure 8. GOES derived TPW difference maps from 13 April 2006

b) Incorporate AIRS sounder products into the NCEP-based WRF/GSI system: This work, proposed to be done in collaboration with ERSL, was intended to accelerate the use of HES in conventional NWP and was scheduled to become more active later in the year. Due to lack of funding for this work at ERSL and the cancellation of HES, resources for this work are being redirected to pre-ABI related activities.

c) Use of POES satellites in nowcasting: AIRS data for the 13April 2006 hail case have been processed with both the standard AIRS processing and CIMSS processing. Preliminary results show major improvement in CIMSS data over land. Tests using these higher-vertical resolution data in nowcasts are planned for the near future.

d) Interact with NWS/WFOs, NSL and NCEP/SPC to evaluate new objective nowcasting products: Initial discussions have begun with NWS/GRB. An overview seminar is being scheduled for this winter based on the fully functional web page, including discussions of quantifying the usefulness of the products and presentation methods for next years severe storm season. Based on the case study results discussed above, GRB suggests that the discussion be expanded to include NWS offices at Sullivan, LaCrosse, Minneapolis and Marquette in the testing.

3) Results of the 13 April 2006 Hail case and preliminary results of the GOES-AIRS data

coverage intercomparisons were presented the August SPIE meeting in San Diego. The presentation "An objective nowcasting tool that optimizes the impact of satellite derive sounder products in very-short-range forecasts" can be found in "Proceedings of SPIE Optics and Photonics 2006 -- Volume 6301 Atmospheric and Environmental Remote Sensing Data Processing and Utilization II: Perspective on Calibration/Validation Initiatives and Strategies, Allen H. L. Huang, Hal J. Bloom, Editors, 63010G (Sep. 1, 2006)".

Task 3. Preparation for Data Assimilation
Lead Investigators: Allen Huang, Xiolie Zhou

Combining multi-channel satellite infrared radiance observation with GPS ROs:
The first type of experiments involves assimilating all AIRS channels in an attempt to ascertain if the full spectrum of AIRS data provides the same, more, or less information regarding the vertical structure of the atmosphere, when compared to the combination of GPS and AIRS data. The second type of experiments involve assimilating a subset of the AIRS data in an attempt to capture the same vertical variability afforded by the assimilation in the first set of experiments.

Figures 9 and 10 show the root mean square error (RMSE) and the correlation between simulated and observed brightness temperatures (BTs) for the selected channels from the NOAA/NESDIS scheme and the adjoint scheme, respectively. The rms error for the NOAA/NESDIS selection appears to have a slight spike in error for channels near the 300 hPa level, whereas the adjoint selected channels do not. The rms error from both selections is less than 3.0 K. The correlations are nearly identical for the channels selected. The reason for this is not entirely clear, but may have something to do with the quality control procedures incorporated into the adjoint selection. Unlike the NOAA/NESDIS selection (which is constant for the entire AIRS domain) the adjoint selection incorporates a clear-channel search and outlier removal methods that may have acted to choose only those channels with low error for the upper levels. This feature will be examined further to ascertain exactly what is causing the difference here.

From these plots it appears that both channel selection schemes are choosing channels that possess similar information regarding the atmospheric column. The next step will be to test both of these schemes via 1D-Var experimentation and comparing the results to the "control" experiments.

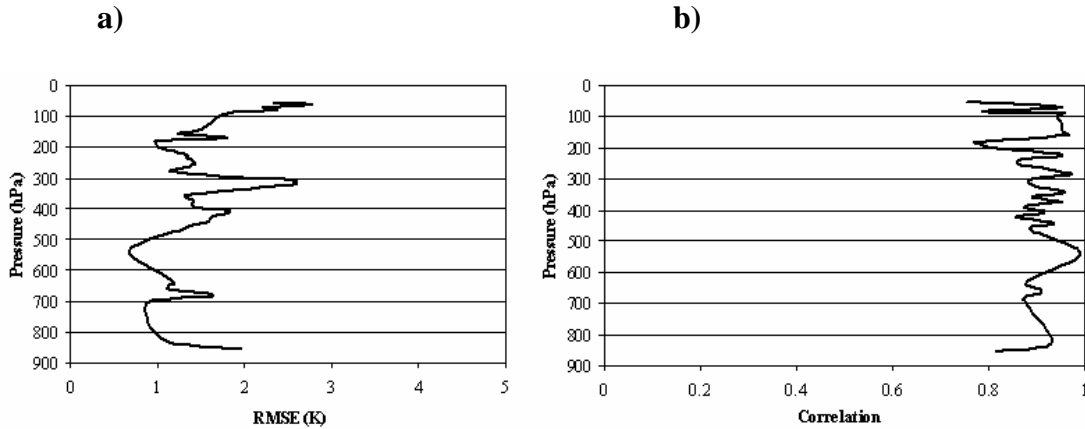a)   b)

Figure 9: Root mean square error (RMSE, panel a) and correlation (panel b) for those channels selected by NOAA/NESDIS scheme. Values arranged vertically by peak WF height. AIRS data obtained from granule 189 at 1900 UTC 11 July, 2003; MM5/SARTA simulated data generated using MM5 19-hr forecast initialized at 0000 UTC 11 July, 2003.

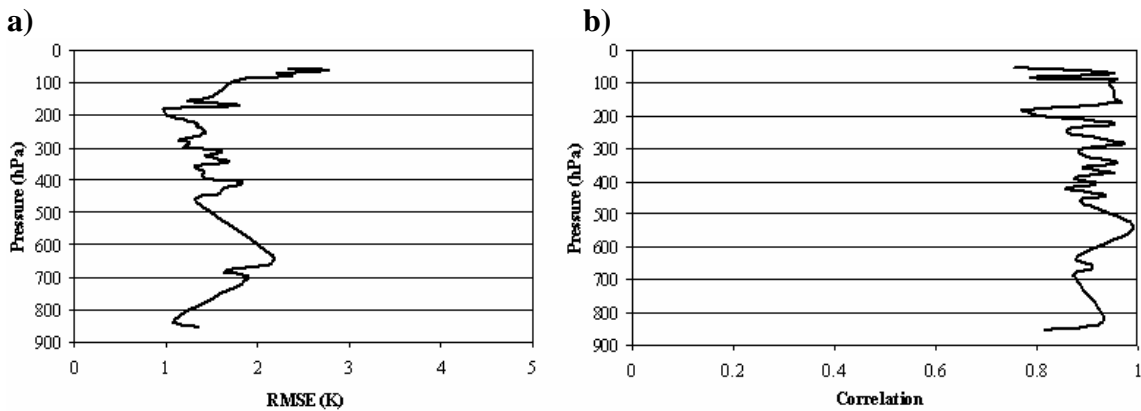a)   b)

Figure 10: Same as in figure 1.1, but for the adjoint sensitivity-based channel selection.

Figure 11 shows the comparison of the observed GPS local refractivity profile (red) to the MM5-GPS operator (MM5/GPS_Op) simulated local refractivity (black) for the G189-Prof2 AIRS and Champ data. The extremely fine vertical resolution of the GPS data can be seen in Fig. 11b, as even the point values are so closely clustered that they still appear as a line. In fact, this particular GPS observation possesses over 2,900 distinct pressure levels ranging from ~3 hPa to 1000 hPa. As can be seen in Fig. 11, below 600 hPa, the model simulated refractivity deviates from the observed values in a pattern not seen in the observations. An inversion appears in the model refractivity profile at about 800 hPa, which is not seen in the GPS RO profile. It is obvious from this that the assimilation of GPS data with AIRS should allow us to obtain a very accurate T and q profiles to be used as the "truth" for the subsequent satellite data assimilation and channel selection studies.
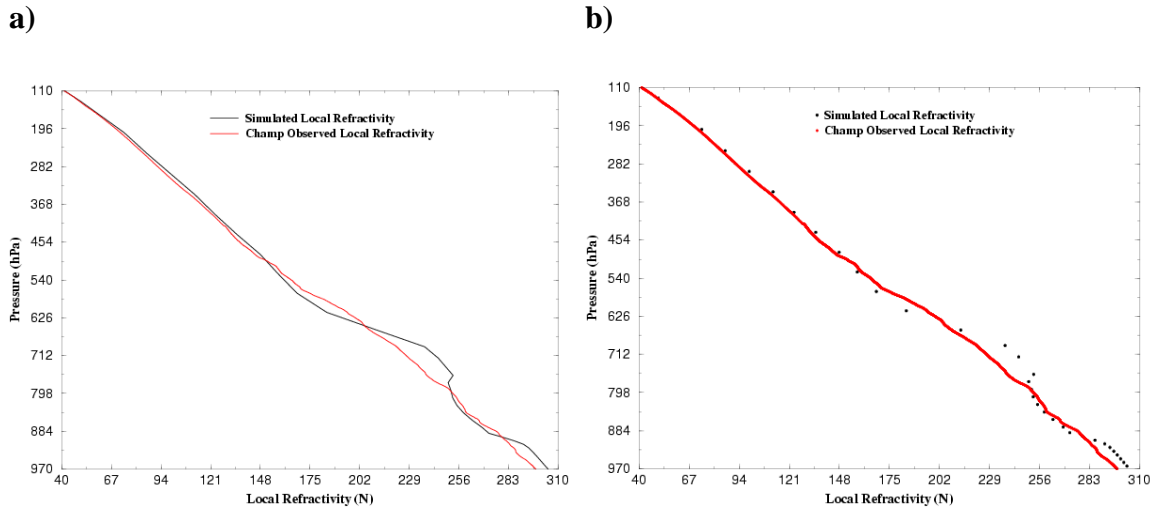
13

Figure 11: Champ observed (red) and MM5/GPS_Op simulated (black) local refractivity (panel a—line, panel b—each individual data point). MM5 data from 16-hr forecast initialized at 0000 UTC 11 July, 2003; Champ refractivity data obtained at 1601 UTC 11 July, 2003.

Observed and modeled vertical variability of the atmosphere
There are several existing channel selection methods for the assimilation of multi-channel infrared radiance observations. We intend to develop a different method aiming at choosing a minimum number of channels that the vertical variability of the atmosphere observed by GIFTS or AIRS is retained. Toward this goal, an EOF analysis is carried out for high-vertical-resolution mixing ratio profiles during convective initiation period. Empirical orthogonal function (EOF) analysis was used to examine the observed vertical structure and vertical variability of water vapor profiles.

In order to accurately describe the mixing ratio at all vertical levels, a certain number of modes should be used. For the CI periods, since some small scale variations often occur in the mixing ratio profiles, a large number of modes are needed to accurately reconstruct the actual profiles. The first 25 mixing ratio eigenvectors are capable of explaining more than 99% of the atmosphere's structure. Thus it is concluded that there are no more than 25 pieces of information about the atmosphere's troposphere and lower stratospheric mixing ratio distribution contained in the convective initialization data set.

Future work includes comparing radiosonde observed vertical variability with that of model forecasts and examining the observed and modeled temporal variability of the atmospheric state. These are necessary and useful information to be used for high-resolution GIFTS data assimilation.

Publication or conference report activity during this period
Carrier, M., X. Zou, and B. Lapenta, 2006: Identifying cloud-uncontaminated AIRS spectra from cloudy FOV based on cloud top pressure and weighting functions. *Mon. Wea. Rev.*, (accepted)

Carrier, M., and X. Zou, 2006: Comparing vertical structures of weighting Function and adjoint sensitivity of radiance and verifying mesoscale forecasts using AIRS radiance observations**.** *Mon. Wea. Rev.*, (to be submitted)

Task 4: GOES-R Ground System Design and Studies
Lead Investigator: Bob Knuteson

The GOES-R Risk Reduction activities related to ground data processing were focused during this quarter on the validation of algorithms for the conversion of raw sensor data to calibrated radiances (L0 to L1). Previous evaluation of algorithms with top of atmosphere simulated GIFTS observations were augmented in this quarter with real observations from the GIFTS Engineering Development Unit at Utah State Space Dynamics Laboratory (SDL). GIFTS data from blackbody calibration targets is being used to evaluate sensor nonlinearity correction algorithms in addition to 2 & 3 body calibration algorithms. During September 2006, a month long collection of GIFTS data samples was collected by SDL under NASA support while viewing the atmosphere from a ground-based configuration coincident with two high accuracy SSEC Atmospheric Emitted Radiance Interferometer (AERI) instruments. This sensor comparison is being used in the validation of SSEC/CIMSS L0 to L1 algorithms developed under NOAA support.

Significant Accomplishments in the last three months
- Draft v0 of GIFTS L0-L1 ATBD presented at GOES-RRR review on August 10.
- Conducted technical interchange meeting with GOES-R Algorithm Integration Team leads at CIMSS on 18-19 September.
- Modified GIFTS L0-L1 resampling algorithm to include a standardized instrument line shape and wavenumber scale.

Plans for Next Three Months
- Verify new GIFTS resampling algorithm and update the GIFTS L0-L1 ATBD.
- Validate the SSEC/CIMSS ground processing algorithms using GIFTS uplooking data.
- Link distributed computing methods, client-server data distribution, and database management to visualization for a web-based concept demonstration.
- Outline a plan for a Level 2 demonstration of water vapor winds processing using simulated Earth observations in a high performance computing environment.

Task 5: Demonstration
Lead Investigator: Dave Tobin

Demonstration / Validation activities within GOES-RRR include demonstration of Level 0-1 and Level 2 algorithms and assessment of product accuracy using algorithms implemented on simulated or proxy datasets. Recent activities have focused on the demonstration of Level 0-1 algorithms on GIFTS sky view radiance data collected (under separate NASA funding) as part of thermal vacuum testing in Logan, UT, which has been recently completed. This includes all aspects of the Level 0-1 algorithm, including, for example, spectral phase alignment, radiometric calibration, and spectral calibration and resampling. This report focuses on progress in demonstration of the spectral algorithms.

Using an FTS and large area Focal Plane Arrays, GIFTS experiences large off-axis effects which must be accounted for in the spectral resampling and calibration algorithms. Spectral resampling is performed to produce output spectra from across the FPAs on a common spectral grid and with common spectral resolution, such that spectra from different pixels in the FPA can be intercompared and a common Radiative Transfer Model and Level 2 algorithm can be applied to all pixels. The spectral resampling algorithm is computationally expensive; current estimates are

that it accounts for approximately 70 percent of the total Level 0-1 computational budget. We have implemented three different algorithms for performing the spectral resampling, and have performed trade-studies in terms of product accuracy and computational efficiency on these three candidate algorithms. The algorithms include 1) interpolation of oversampled spectra to a common wavenumber scale which is based on heritage code developed for our ground based and aircraft FTS sensors, 2) since interpolation accomplished with matrix multiplication which is being used in the CrIS processing, and 3) interpolation of oversampled interferograms to a common optical path difference scale. Approach number 2 has the advantage that the matrix multiplications are very fast computationally; however we have found that pre-computing the required number of resampling matrices is prohibitive with respect to system memory and that computing the matrices on the fly is not efficient. We have recently adopted approach number 3 in the GIFTS Level 0-1 processing. It involves the production of an oversampled interferogram for each pixel, interpolation of the interferogram to a standard optical path difference grid, and FFTing to produce resample spectra. In addition to resampling to a standard wavenumber grid, this approach also normalizes each pixel (spectrum) to a standard spectral resolution. The accuracy and computational efficiency of this critical processing component has been demonstrated. An example for GIFTS sky view data collected in May 2006 as part of the EDU thermal vacuum characterization tests is shown in Figure 12.
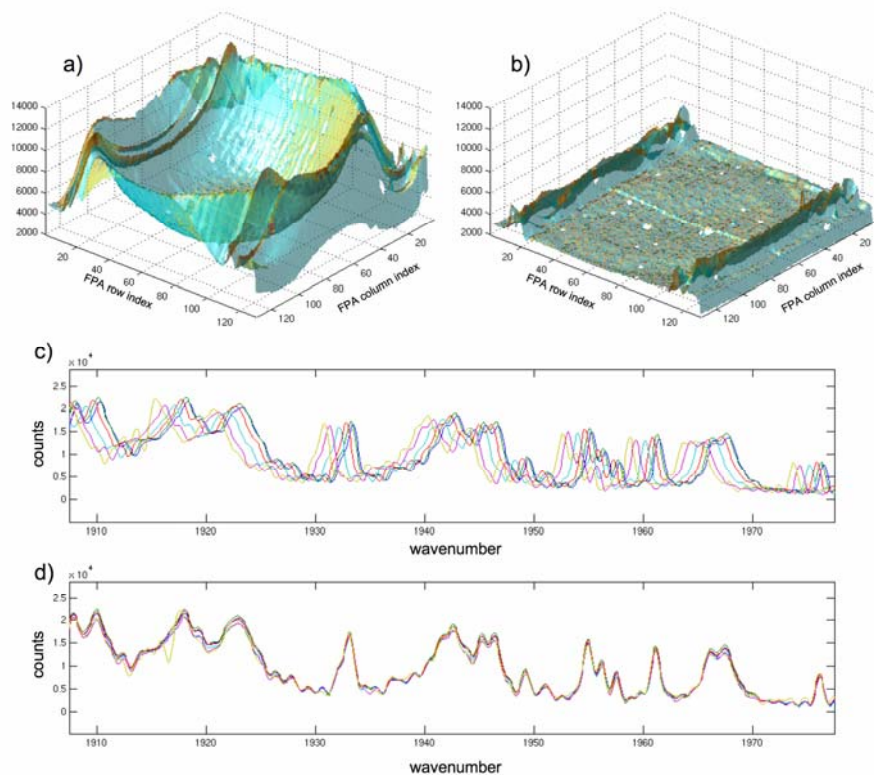

Figure 12. Demonstration of the Level 0-1 spectral calibration and spectral resampling algorithms for GIFTS EDU sky view data. Panel a) shows raw count data (not radiometrically calibrated) for a fixed spectral bin before spectral processing. The approximately circular symmetric off-axis effects causing pixels across the FPA to sample different wavenumbers are evident. Panel b) shows the same data but after spectral calibration and resampling. The off-axis effects have been removed. (Other effects, however, related to readout noise and vignetting, are also seen). Panels c) and d) display sample sky view data along the FPA diagonal before (panel c) and after (panel d) the spectral processing.

CIMSS Finances Summary: GOES-RRR Funding and Spending Plan

GOES R Risk Reduction <u>Funding</u>		**GOES R Risk Reduction <u>Spending</u>**	
Through 2/2004	$1,270K	Through 2/2004	$1,299K
Through 2/2005	$ 750K	3/2004 - 2/2005	$ 880K
Through 2/2006	$ 910K	3/2005 – 2/2005	$ 645K
Through 9/2006	<u>$1,400K</u>	3/2006 – 9/2006	<u>$ 1,048K</u>
Total funding to date	$4,330K	Total spending thru 12/31/05	$ 3,872K